논문 2008-45IE-2-3

플라나 마이크로스트립 전송선의 효율적 해석 방법

(An Efficient Analysis Method for Planar Microstrip Transmission Line)

김 태 원*

(Tae-Won Kim)

요 약

TLM 수치 해석법의 주요한 장점은 가장 복잡한 전송선 구조에 있어서도 해석이 용이하다는 것이다. 본 논문에서는 대칭압축노드를 이용한 TLM법을 마이크로스트립 meander 라인에 성공적으로 적용하였다. 플라나 마이크로스트립 전송선을 모델화하기 위한 대칭압축노드에 대한 상세한 기술이 제시되었고 또한 2종류의 마이크로스트립 meander 라인의 산란 파라메터 S_{11}과 S_{21}을 계산하였다. 구해진 결과로부터 TLM 해석법이 복잡한 플라나 마이크로웨이브 전송선 구조를 모델링하는데 유용한 해석법임을 보였다. 제시된 TLM 해석 결과는 고주파 영역에서 마이크로웨이브 집적 회로를 설계하는데 유용하게 사용될 수 있다.

Abstract

The main advantage of the TLM analysis method is the ease with which even the most complicated transmission line structures. In this paper, using symmetrical condensed node(SCN), the TLM numerical technique has been successfully applied to microstrip meander line. A detailed technique of the symmetrical condensed node(SCN) may be used to model planar microstrip transmission line is presented. Also, the S-parameters S_{11} and S_{21} of two types of microstrip meander line have been computed. From obtained results, TLM analysis is shown to be an efficient method for modeling complicated structure of planar microstrip transmission line. The TLM results presented here are useful in the design of microwave integrated circuits at higher frequencies region.

Keywords : TLM, symmetrical condensed node(SCN), microstrip meander line, planar

I. Introduction

Analysis, modeling, and design of transmission lines are important for any component and subsystem development. And then numerical analysis for microwave transmission line structures under study is needed for computer simulation of circuits in communication systems. All field solution techniques, whether analytical, graphical, or numerical, serve the same purpose, namely to find solutions of Maxwell's equations that satisfy the boundary conditions.

Various analytical and numerical methods such as Fourier integral method[1], mode matching method[2~3], spectral domain method[4], the boundary element method[5] and the finite element method[6] have been used to obtain characteristics data. But these analytical and numerical methods cannot be easily applied to irregularities transmission line in the structures and discontinuities of arbitrary cross section. The TLM method is one of the most powerful solvers of electromagnetic problems. Because in TLM method the analytical pre-processing in almost negligible, and the basic

* 평생회원, 상지영서대학 국방정보통신과
(Department of Military Defense Information and Communication, Sangji Youngseo College)
접수일자: 2008년3월4일, 수정완료일: 2008년6월5일

algorithms are easily modified to solve any kind of electromagnetic problem, either irregular structure or discontinuities of arbitrary cross section. Unlike other numerical methods which are based on the discretization of Maxwell's equations, the TLM method[7~8] embodies Huygens's principle in discretized form. Also, attached to the nodes are a number of stubs whose electrical properties are used to represent the electrical characteristics of the propagation space. The numerical process then entails determining the impulse response of this equivalent network and taking the Fourier transform of the output response function to obtain the spectral domain solution.

In this paper, the frequency dependent scattering parameters have been investigated for two types of microstrip meander line using TLM method. and then frequency domain response for microstrip meander line are obtained. From obtained results, TLM analysis is shown to be an efficient tool for modeling complicated structure of planar microwave transmission line.

II. Scattering process in TLM method

The symmetrical condensed node(SCN) has been well established for the solution of electromagnetic field problems in three dimensions. The SCN node is shown in fig. 1. This is a unit cell of the generalized 3-D TLM network and the SCN node has been developed by P. B. Johns.[9] The SCN node consists of twelve ports and is augmented by three capacitive and three inductive stubs to model inhomogeneous materials. It is based on enforcing continuity of the electric and magnetic fields and conservation of charge and magnetic flux.

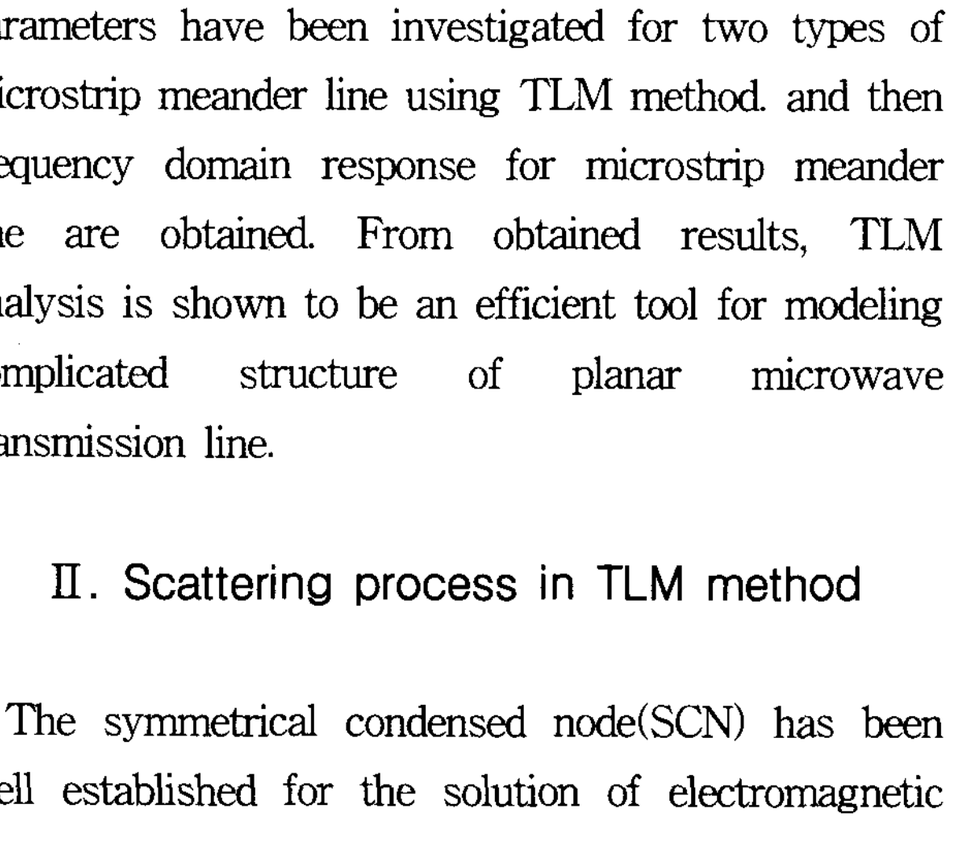

그림 1. 대칭압축노드
Fig. 1. Symmetrical Condensed Node(SCN).

In fig. 1, the first subscript indicates the direction of propagation(x, y, z). The second subscript is either n or p to indicate a line segment along negative or positive axis. The third subscript is indicates the direction of polarization of the voltage pulse. As shown in fig.1, by equalizing the sum of charges and flux on each lines to that in the center of the node and solving for V_y, I_z it follows that

$$V_y = \frac{Y_{xny} V_{xny} + Y_{xpy} V_{xpy}}{Y_{xny} + Y_{xpy}} \tag{1}$$

$$I_z = \frac{Z_{xpy} I_{xpy} + Z_{xny} I_{xny}}{Z_{xny} + Z_{xpy}} \tag{2}$$

Expressing the total voltage in terms of the incident and reflected voltages and using the equality

$$\frac{Y_1}{Y_1 + Y_2} = \frac{Z_2}{Z_1 + Z_2} \tag{3}$$

Equation (1) and (2) can be rewritten as

$$V_y = \frac{Z_{xny}}{Z_{xny} + Z_{xpy}} (V_{xpy}^i + V_{xpy}^r) + \frac{Z_{xpy}}{Z_{xny} + Z_{xpy}} (V_{xny}^i + V_{xny}^r) \tag{4}$$

$$I_z = \frac{1}{Z_{xny} + Z_{xpy}} (V_{xpy}^i - V_{xpy}^r) - \frac{1}{Z_{xny} + Z_{xpy}} (V_{xny}^i - V_{xny}^r) \tag{5}$$

Multiplying equation (5) by Z_{xny}, adding it to equation (4), and solving for V_{xny}^r and then the reflected voltage pulse on the other side of the node center V_{xpy}^r can be derived by multiplying equation (5) by Z_{xny}. After solving for V_{xny}^r and V_{xpy}^r it

follows that

$$V^r_{xny} = V_y + I_z Z_{xny} + \frac{Z_{xny} - Z_{xpy}}{Z_{xny} + Z_{xpy}} V^i_{xny} - \frac{2Z_{xny}}{Z_{xny} + Z_{xpy}} V^i_{xpy} \quad (6)$$

$$V^r_{xpy} = V_y - I_z Z_{xpy} + \frac{Z_{xpy} - Z_{xny}}{Z_{xny} + Z_{xpy}} V^i_{xpy} - \frac{2Z_{xpy}}{Z_{xny} + Z_{xpy}} V^i_{xny} \quad (7)$$

Scattering equation (6) and (7) can be written as

$$V^r_{xny} = V_y + I_z Z_{xny} - V^i_{xpy} + h_{xy} \quad (8)$$

$$V^r_{xpy} = V_y - I_z Z_{xpy} - V^i_{xny} + h_{xy} \quad (9)$$

where h_{xy} is defined as

$$h_{xy} = \frac{Z_{xny} - Z_{xpy}}{Z_{xny} + Z_{xpy}} (V^i_{xny} - V^i_{xpy}) \quad (10)$$

Finally, y directed equivalent total voltage V_y and equivalent total current I_z solely in terms of incident voltages as follows.[10]

$$V_y = 2\frac{Y_{xny}V^i_{xny} + Y_{xpy}V^i_{xpy} + Y_{zny}V^i_{zny} + Y_{zpy}V^i_{zpy} + Y_{oy}V^i_{oy}}{Y_{xny} + Y_{xpy} + Y_{zny} + Y_{zpy} + Y_{oy} + G_{ey}} \quad (11)$$

$$I_z = 2\frac{V^i_{xpy} - V^i_{xny} + V^i_{ynx} - V^i_{ypx} - V^i_{sz}}{Z_{xny} + Z_{xpy} + Z_{ynx} + Z_{ypx} + Z_{sz} + R_{mz}} \quad (12)$$

Subsequently, voltage pulse reflected to th link lines and stubs can be computed by making use of scattering equations (8) and (9). Using similar procedure, the scattering equation in SCN node is applied to all the lines in incident voltage pulses. Also, in the TLM numerical analysis, the scattering of the voltage pulses at the center of the SCN node is represented by the scattering matrix. A simple scattering process can be used to determine the scattering matrix. The scattering expression of entire domain under the studying objects is as follows.[9~10]

$$V^r = S\ V^i \quad (13)$$

where V^r is reflected voltage and V^i is incident voltage. The ordering of voltage pulses within the scattering matrix S is carried out with respect to the original SCN notation. Because there are no incident voltages from lossy stubs, the scattering matrix S is composed of 24 × 18 or a full 24 × 24 square matrix with zero columns.

Ⅲ. Absorbing boundary condition

For waveguiding structures with inhomogeneous cross section, the absorbing boundary conditions used in this section are very effective[11~12].

$$\begin{aligned} E^n(m,j,k) = {} & (\alpha_1+\alpha_2)E^{n-1}(m,j,k) - \\ & \alpha_1\alpha_2 E^{n-2}(m,j,k) + (\beta_1+\beta_2)E^n(m,j,k) + \\ & (\gamma_1+\gamma_2-\alpha_1\beta_2-\beta_1\alpha_2)E^{n-1}(m-1,j,k) - \\ & (\alpha_1\gamma_2+\gamma_1\alpha_2)E^{n-2}(m-1,j,k) - \\ & \beta_1\beta_2 E^n(m-2,j,k) - (\beta_1\gamma_2+\gamma_1\beta_2) \\ & E^{n-1}(m-2,j,k) - \gamma_1\gamma_2 E^{n-2}(m-2,j,k) \end{aligned} \quad (14)$$

where α_i, β_i and γ_i are interpolation coefficients.

$$\alpha_i = \frac{a - g_i(1-b)}{a - 1 - g_i(1-b)},\ \beta_i = \frac{a - 1 + g_i b}{a - 1 - g_i(1-b)},$$

$$\gamma_i = \frac{-a - bg_i}{a - 1 - g_i(1-b)}$$

and $a = b = 0.5;\ g_i = 2\sqrt{\epsilon_{eff}}\ ;\ i = 1,2.$

The voltage impulses incident on the absorbing boundary planes are functions of both tangential electric and magnetic fields. Hence the absorbing boundary equation (14) can be applied to the TLM impulses.

Ⅳ. Extraction of S-parameters in analysis objects

In analysis model, the S-parameters extraction process has been made more simple by the application absorbing boundary conditions. Extraction of the reflection coefficient demands separation of the reflected field from the total field and the transmitted

field at the output port. The incident field, V_{inc} is obtained from analysis of a small section of the microstrip substrate terminated at both ends with simulated wideband matched terminations. The total field, V_{tot} are obtained from analysis of the circuit with discontinuity present. From the incident and reflected fields it is straightforward to compute the S-parameters. The expression of S-parameter is as follows[13]

$$S_{11} = \frac{V_{tot} - V_{inc}}{V_{inc}} \tag{15}$$

$$S_{21} = \frac{V_{trans}}{V_{inc}} \tag{16}$$

In this case the input and the output port are assumed to have the same impedance so that the information on the field alone sufficed to compute the S-parameters.

V. Numerical results

In order to compute the S-parameters of a microstrip meander line, the information of the incident and reflected fields at the input port and the transmitted field at the output port is needed. The geometry of the two types of microstrip meander line is shown in fig. 2. The microstrip thickness is assumed to be zero and the relative dielectric constant of the substrate is 9.2. The number of iterations was 4200. To model a microstrip meander line properly, a finer mesh should be implemented at the area which surrounds the edge.

The SCN cubic cell results have been obtained with the discretization $\Delta x = \Delta y = \Delta z = 0.025mm$. The incident voltage, 1V peak value generated by the electric source. When impulses are excited into the analysis objects, they are scattered at nodes and boundaries of entire domain and arrive after some time at the input and output reference planes.

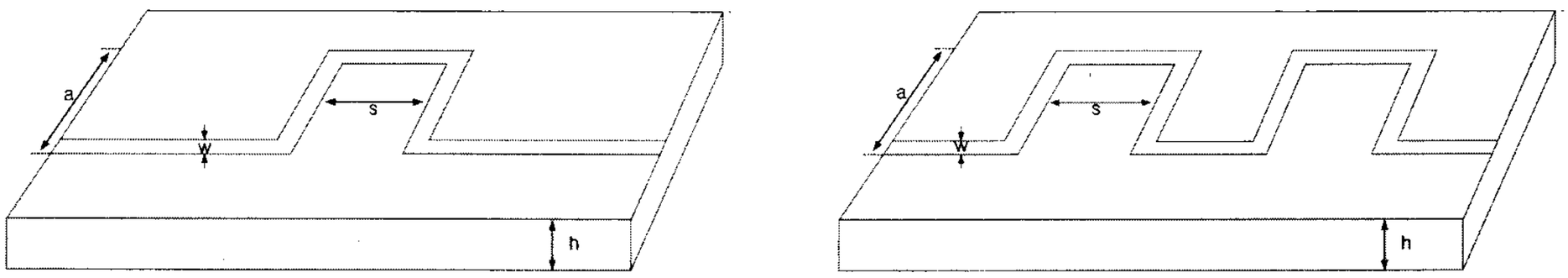

(a) A형 (b) B형
(a) Type A (b) Type B

그림 2. 마이크로스트립 meander 라인 ($h = 0.6mm,\ w = 1.5mm,\ a = 6.0mm,\ s = 4.0mm$)
Fig. 2. Schematic of microstrip meander line.($h = 0.6mm,\ w = 1.5mm,\ a = 6.0mm,\ s = 4.0mm$)

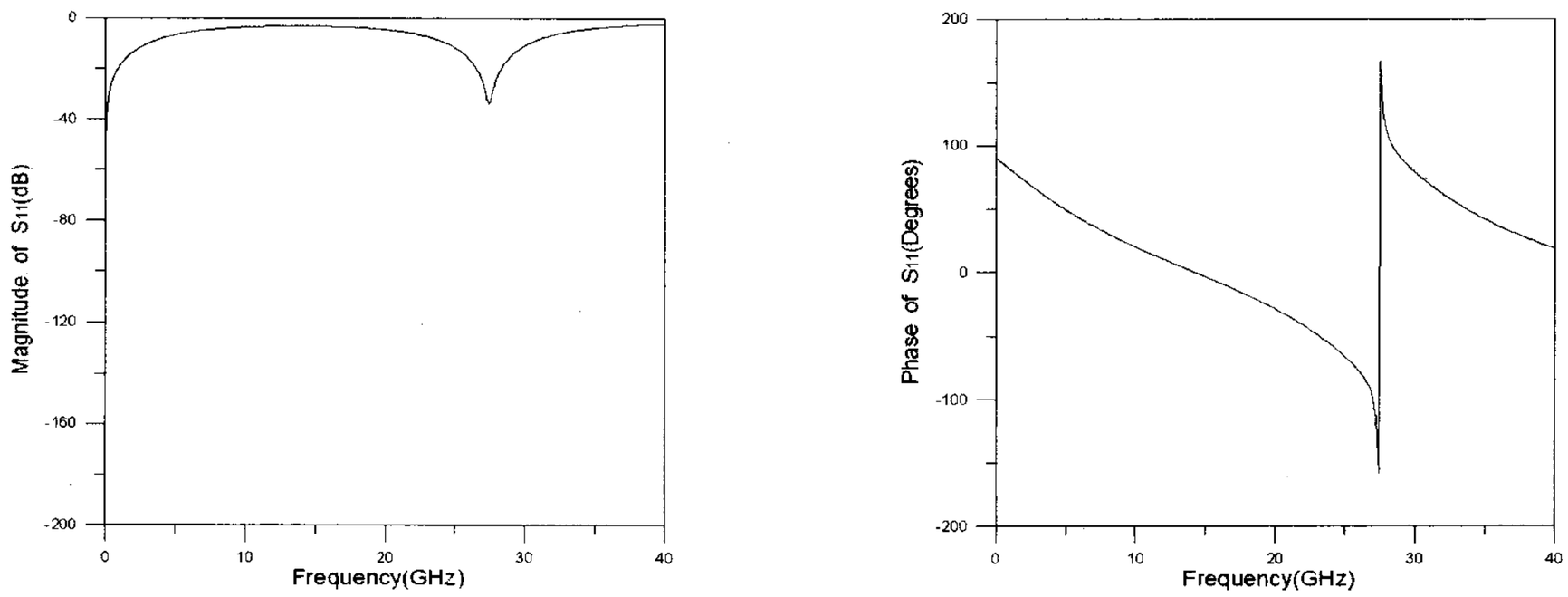

(a) 크기 (b) 위상
(a) Magnitude (b) Phase

그림 3. 그림 2에서 A형 마이크로스트립 meander 라인의 S_{11}
Fig. 3. S_{11} of Microstrip Meander line for type of A in fig. 2.

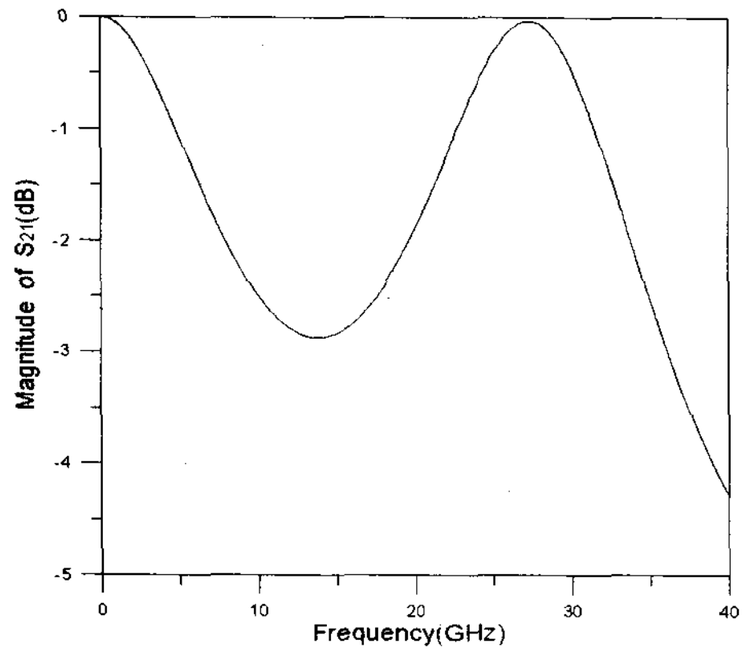

(a) 크기
(a) Magnitude

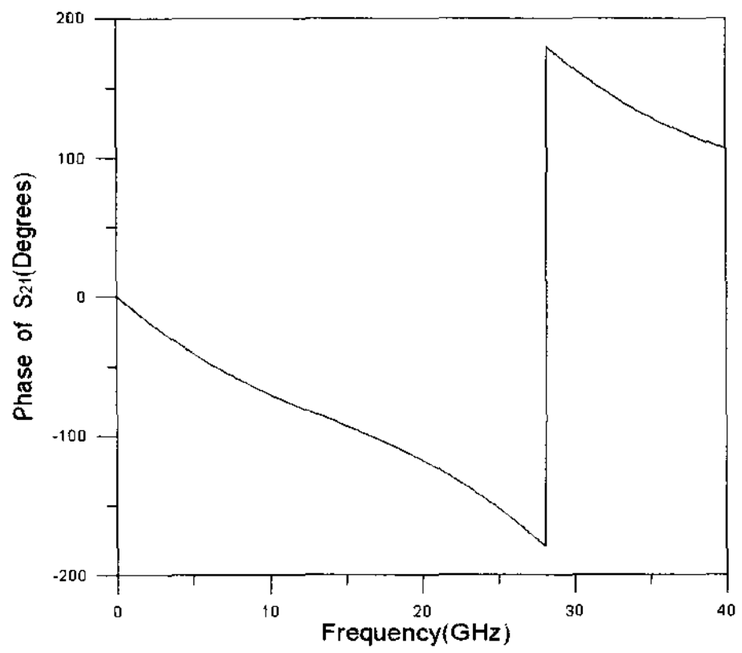

(b) 위상
(b) Phase

그림 4. 그림 2에서 A형 마이크로스트립 meander 라인의 S_{21}
Fig. 4. S_{21} of Microstrip Meander line for type of A in fig. 2.

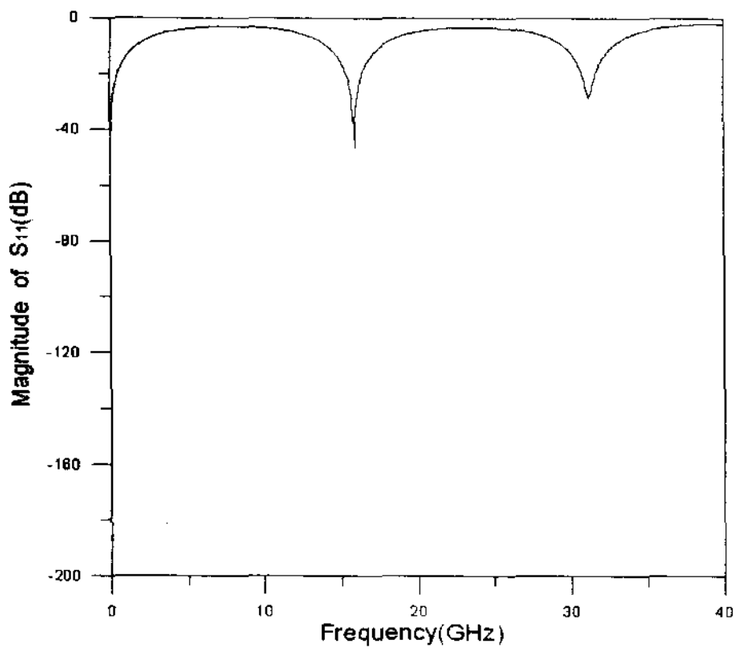

(a) 크기
(a) Magnitude

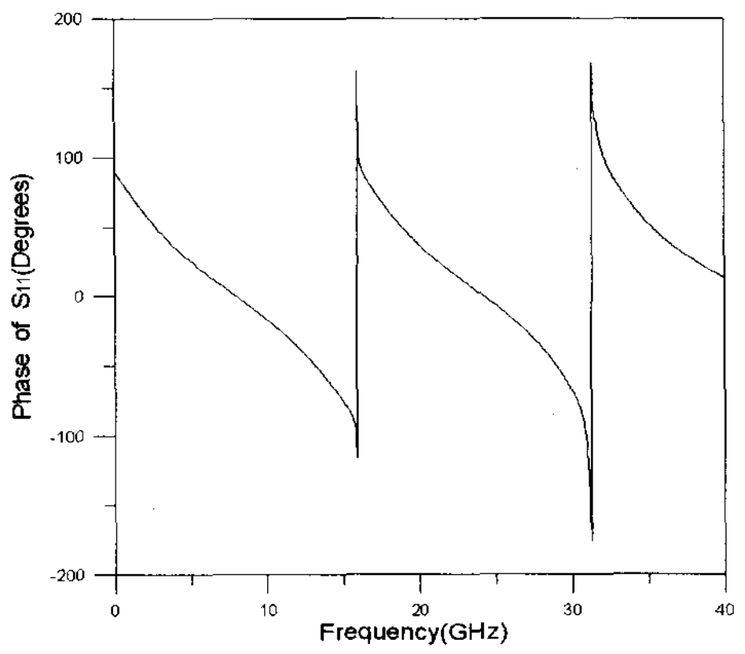

(b) 위상
(b) Phase

그림 5. 그림 2에서 B형 마이크로스트립 meander 라인의 S_{11}
Fig. 5. S_{11} of Microstrip Meander line for type of B in fig. 2.

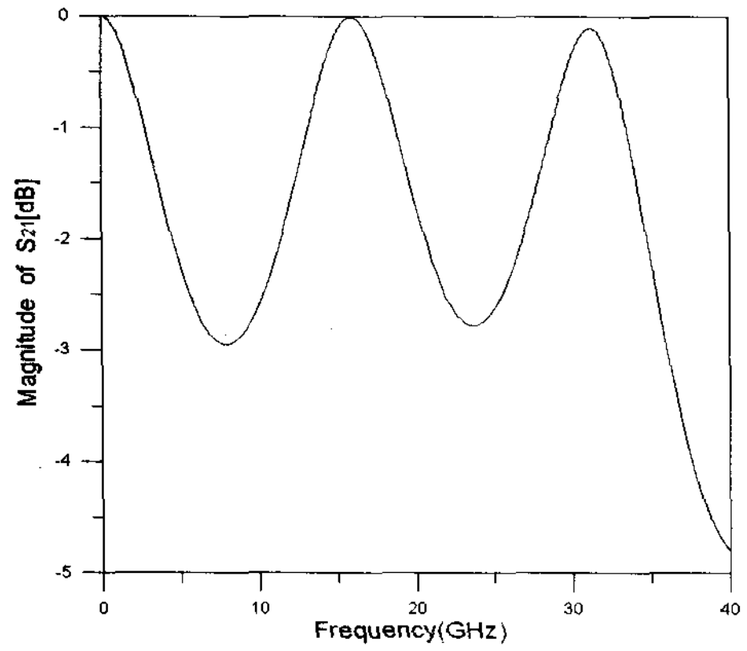

(a) 크기
(a) Magnitude

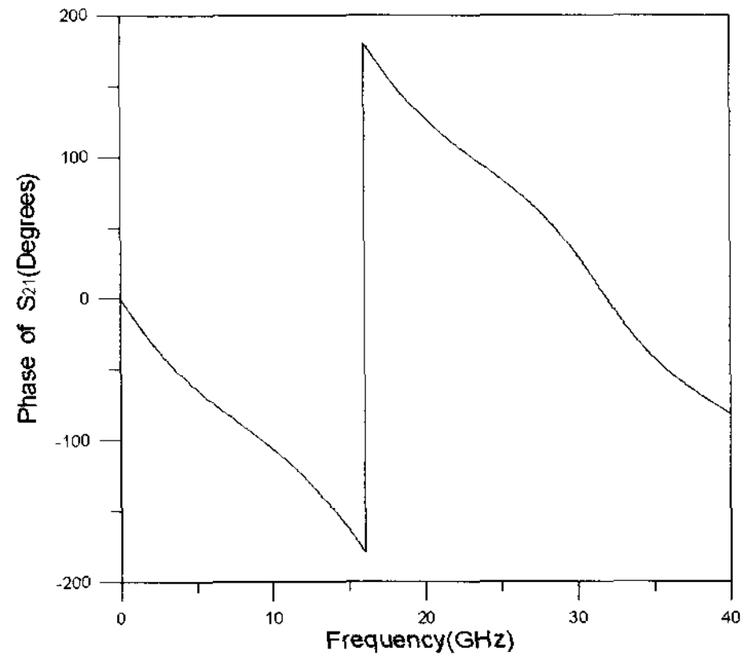

(b) 위상
(b) Phase

그림 6. 그림 2에서 B형 마이크로스트립 meander 라인의 S_{21}
Fig. 6. S_{21} of Microstrip Meander line for type of B in fig. 2.

The absorbing boundary condition are applied at the two ends of the microstrip meander lines. This absorbing boundary condition has very low reflections over a wide frequency band. The computed S-parameters for a microstrip meander line about type of A are plotted in fig. 3. and fig. 4. Also, the S-parameters for a microstrip meander line about type of B are plotted in fig. 5. and fig. 6. The computed results a well expressed for a characteristics of microstrip meander line. But the cubic TLM node is coarser than the other TLM node. It is well known that the electric field varies fast at edges of a microstrip meander line structure. The fine discretization for the smaller coarseness is needed to well represent the field in those areas. However, the errors associated with the TLM analysis, such as coarseness error, velocity error are negligible for this cell size.

VI. Conclusion

The main advantage of the TLM numerical analysis is the ease with which even the most complicated structures. The great flexibility and versatility of the numerical method reside in the fact that the TLM network incorporates the properties of electromagnetic fields and their interaction with the boundaries and materials. In this paper, the TLM numerical technique has been successfully applied in microstrip meander line. Using absorbing boundary condition, the S-parameters S_{11} and S_{21} of two types of microstrip meander line have been computed, and no ripple is detected in either magnitude or phase response. Also, a interpolation technique based on the dominant field has been proposed for efficient S-parameters extraction. The TLM results presented here are useful in the design of microwave integrated circuits. In addition, the TLM modelling becomes a useful tool for the improvement of existing analytical CAD models at higher frequencies. In the future, in order to increase the numerical efficiency and reduce the various errors associated with the TLM modelling, more programming effort and the new SCN node must be investigated.

References

[1] A. El-Sherbiny, "Exact Analysis of Shielded Microstrip Lines and Bilateral Finlines", *IEEE Trans. Microwave Theory Tech.*, vol. MTT-29, pp. 669-675, July 1981.

[2] J. Bornemann and F. Arndt, "Calculating the Characteristic Impedance of Finlines by Transverse Resonance Method", *IEEE Trans. Microwave Theory Tech.*, vol. MTT-21, pp. 85-92, Jan. 1986.

[3] R. Sorrentino and T. Itoh, "Transverse Resonance Analysis of Finline Discontinuities", *IEEE Trans. Microwave Theory Tech.*, vol. MTT-32, pp. 1633-1638, Dec. 1984.

[4] L. P. Schmidt and T. Itoh, "Spectral Domain Analysis of Dominant and Higher Modes in Finlines", *IEEE Trans. Microwave Theory Tech.*, vol. MTT-28, pp. 981-985, Sept. 1980.

[5] S. Kagami and I. Fukai, "Application of Boundary Element Method to Electromagnetic Field Problems", *IEEE Trans. Microwave Theory Tech.*, vol. MTT-32, pp. 455-461, April. 1984.

[6] P. Silvester, R. L. Ferrari, "*Finite Element for Electrical Engineers*", Cambridge University Press, Cambridge 1983.

[7] P. B. Johns,"A Symmetrical Condensed Node for the TLM Method," *IEEE Trans. Microwave Theory Tech.*, vol. MTT-35, pp. 370-377, April. 1987.

[8] Poman So, Eswarappa, and Wolfgang J. R. Hoefer, "A Two-Dimensional TLM Microwave Simulator Using New Concepts and Procedures", *IEEE Trans. Microwave Theory Tech.*, vol. MTT-37, pp. 1877-1884, Dec. 1989.

[9] P. B. Johns, "A Symmetrical Condensed Node for the TLM Method," *IEEE Trans. Microwave Theory Tech.*, vol. MTT-35, pp. 370-377, Sept. 1987.

[10] V. Trenkic, "The Development and Characterization of Advanced Nodes for the TLM Method", Ph. D. Thesis, University of Nottingham, UK, Nov. 1995.

[11] C. Eswarappa and Wolfgang J. R. Hoefer, "One-Way Equation Absorbing Boundary Conditions for 3D TLM Analysis of Planar and Quasi-Planar Structures," *IEEE Trans.*

Microwave Theory Tech., vol. MTT-42, pp. 1669-1677, Sept. 1994.
[12] R. L. Higdon, "Numerical Absorbing Boundary Conditions for the Wave Equation," *Math Comp.*, vol. 49, no. 179, pp. 65-91, July. 1987.
[13] Eswarappa, George I. Costache and Wolfgang J. R. Hoefer, "Transmission Line Matrix Modeling of Dispersive Wide-Band Absorbing Boundaries with Time Domain Diakoptics for S-Parameter Extraction," *IEEE Trans. Microwave Theory Tech*, vol. MTT-38, pp.379-385, April. 1990.

저 자 소 개

김 태 원(평생회원)
1986년 청주대학교 전자공학과 학사 졸업.
1990년 중앙대학교 대학원 전자공학과 석사 졸업.
1997년 중앙대학교 대학원 전자공학과 박사 졸업.
1997년~현재 상지영서대학 국방정보통신과 교수
<주관심분야 : 초고주파, RF회로 설계, 안테나>